Power-Amplifier Stabilization Through Out-of-Band Feedback

William Sear, *Graduate Student Member, IEEE*, and Taylor W. Barton, *Senior Member, IEEE*

***Abstract*— This letter presents a power-amplifier (PA)-stabilization technique based on the low-frequency out-of-band feedback. The proposed structure replaces a conventional stability network to ensure unconditional stability at the frequencies up to the radio-frequency (RF) operating band, with the in- and above-band frequencies stabilized through the matching network design. The approach offers an alternative to inserting the lossy components in the RF signal path, which can significantly degrade the realizable in-band gain of the amplifier. The 900-MHz proof-of-concept PA based on a 10-W gallium-nitride (GaN) device is characterized under the continuous-wave (CW) and Wideband Code Division Multiple Access signal (W-CDMA) excitations and realizes 25.6-dB small-signal gain and 73% power added efficiency (PAE) at P3dB.**

***Index Terms*— Baseband, gallium nitride (GaN), power amplifiers (PAs), radio frequency (RF), stabilization.**

I. Introduction

POWER-amplifier (PA) stability is a nonnegotiable requirement among a performance trade space of gain, linearity, efficiency, and bandwidth. Stability is typically ensured by the stabilization networks incorporated into the input match and the gate bias line and designed to suppress the frequency-dependent gain of the device in and/or out of band, thus preventing the oscillations caused by the nonunilateral nature of the device [1]. While the out-of-band gain reduction does not incur a performance penalty, the stability network inevitably also degrades the in-band gain due to its insertion loss.

In this letter, we demonstrate a new approach to single-stage PA stabilization, which eliminates the need for a conventional stability network. A low-frequency feedback network is embedded in the gate and drain bias lines of the PA to control the stability response up to the radio-frequency (RF) operating frequency. This approach produces a stable PA without the need for lossy elements in the RF signal path, realizing a PA gain closer to the GMax of the device [2]. A stabilization network connecting the bias networks together in out-of-band feedback has not been previously demonstrated and represents a novel approach to stabilization. While resistive feedback is employed in some amplifiers at the expense of gain [3], [4], by restricting the compensation to out of band, the RF performance of the device is not compromised.

Manuscript received May 20, 2020; accepted June 11, 2020. Date of publication June 24, 2020; date of current version August 7, 2020. This work was supported by the National Science Foundation under Grant 1846507. *(Corresponding author: Taylor W. Barton.)*

The authors are with the Department of Electrical, Computer, and Energy Engineering, University of Colorado at Boulder, Boulder, CO 80309 USA (e-mail: william.sear@colorado.edu; taylor.w.barton@colorado.edu).

Color versions of one or more of the figures in this letter are available online at http://ieeexplore.ieee.org.

Digital Object Identifier 10.1109/LMWC.2020.3002727

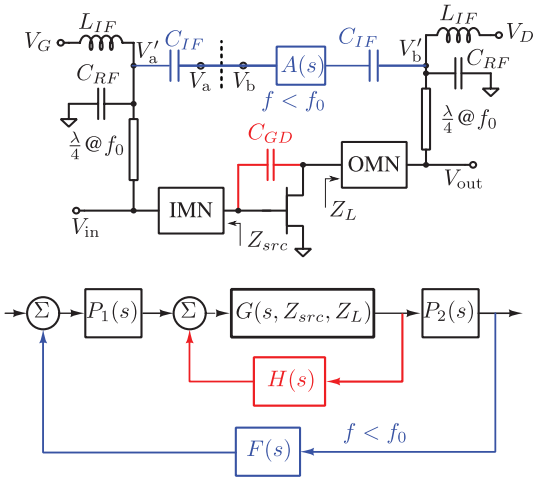

Fig. 1. Equivalent circuit and block diagram of the out-of-band feedback stabilized PA. The forward path "plant" comprises the transistor and passive matching network ($P_1(s)$ and $P_2(s)$) responses, including the internal transistor feedback $H(s)$. The feedback transfer function $F(s)$ combines the effects of the coupling network and filter $A(s)$ and is designed as low pass to avoid perturbing the RF signal path.

The proposed technique is demonstrated here with a 900-MHz prototype single-stage PA. We note that we use the conventional small-signal assumptions under which the k-factor applies, as is typical in the single-stage PA design. Analysis treating parametric oscillations requires nonlinear techniques that are the subject of significant research interest [5] but are a category of the stability problem outside the scope of this letter.

II. Theory

We treat PA stability in three distinct regions of operation: below the operating band, where the out-of-band feedback will operate; within the operating band, where conditional stability is allowed [1]; and above the band, where unconditional stability is ensured through the output matching network design. The single-stage PA is modeled as shown in Fig. 1, where the transistor is treated as a frequency-dependent forward gain path with a local feedback path dominated by C_{gd}. The gain of this "plant" is also dependent on the impedances presented at the source and the load by the input and output matching networks (IMN and OMN). In-band and above band (i.e., for $f \geq f_0$), the system behaves as a standard RF PA. At frequencies below f_0, we introduce a feedback network, $F(s)$, to control the stability, treating the existing PA as a minor loop.

The prototype PA design, described in detail in Section III, is based around the large-signal model of the packaged

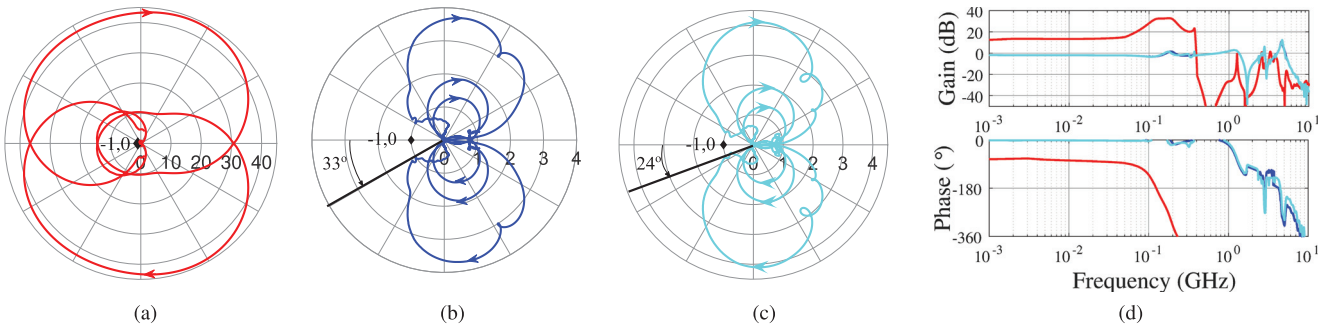

Fig. 2. Simulated Nyquist plots based on the large-signal model under small-signal excitation. (a) Base PA without feedback, terminated in the nominal 50-Ω $Z_{L,\text{src}}$. (b) PA with feedback, terminated in the nominal $Z_{L,\text{src}}$. (c) PA with feedback and with the RF input and outputs terminated in $Z_{L,\text{src}} = 0.1 + j50\ \Omega$. (d) Bode plots of the three cases.

CG2H40010F device from Wolfspeed, making exact expressions for $G(s)$ and $H(s)$ unknown. Therefore, Nyquist stability analysis based on the simulated loop transfer functions formulated as voltage ratios is an appropriate tool [6]. To ensure minor loop stability and stability above the operating frequency of the feedback loop $H(s)$, the matching networks of the base PA (i.e., without feedback) are designed to ensure there will be no right-half-plane (RHP) poles. In practice, this means that the IMN and OMN are designed without high-Q resonant networks. Fig. 2(a) shows the simulated transfer function of the forward path, i.e., the voltage ratio V_b'/V_a' referring to Fig. 1, when the RF input and output ports are terminated in 50 Ω. Because there are no RHP poles in the forward path, the four encirclements of the -1 point indicate an unstable system [6].

To correct the instability, a feedback path is introduced through the coupling capacitor C_{IF} and the transfer function $A(s)$ [Fig. 1]. The $A(s)$ network is designed to modify the loop transfer function such that the negative x-axis crossings in the Nyquist domain occur to the right of the -1 point, eliminating the encirclements. In general, this can be accomplished through an appropriate combination of attenuation, lead, and/or lag networks [6]. Here, $A(s)$ is a 30-dB attenuator with a third-order resonant low-pass filter to ensure that its roll-off occurs at approximately 300 MHz, below the RF operating frequency. We note that the overall transfer function $F(s)$ is determined by a combination of $A(s)$ and the coupling networks C_{IF} and L_{IF} [Fig. 1]. The combined low-pass natures of these transfer functions mean that the PA behavior will be unaffected above the $F(s)$ cutoff frequency—here approximately 300 MHz.

The effect of the feedback can be observed in Fig. 2(b), which shows the Nyquist plot when the feedback is included, and in the corresponding Bode plot in Fig. 2(d). We note that these figures show the closed-loop transfer function, V_b/V_a (Fig. 1), and not the RF forward voltage gain, $V_{\text{out}}/V_{\text{in}}$, of the PA. With the feedback, the system becomes stable with a phase margin of 33° when the RF input and output are terminated in the nominal 50 Ω. Stability is also evaluated for an example case, where the input and output are reactively terminated ($Z_{\text{src}} = Z_L = 0.1 + j50\ \Omega$) [7]. This case is shown in Fig. 2(c) and (d), indicating a stable loop response with a 24° phase margin.

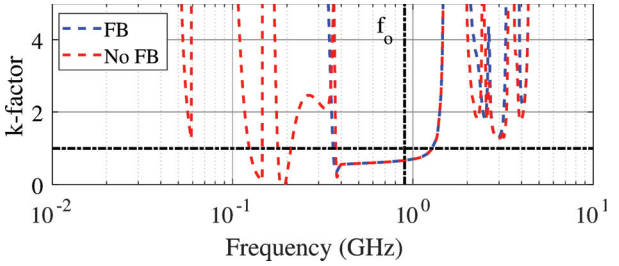

Fig. 3. Simulated k-factor with and without feedback.

Unconditional stability in response to the source and load variations is generally described using the k-factor, and the addition of the feedback path $F(s)$ does not invalidate this analysis technique. The k-factors for the PA with and without feedback are compared in Fig. 3 over the valid frequency range of the device model. In addition to the feedback enforcing $k > 1$ up to the operating frequency, an improvement in the in-band is observed for the PA with feedback, which is attributed to the loading effects of C_{IF}. Because the terminations will be well controlled over the operating frequency range, conditional stability is allowed from 300 to 1050 MHz. Above this band, the device gain combined with the losses in the IMN and OMN produces unconditional stability.

III. Prototype Design and Measurement

A 900-MHz PA based on the CG2H40010F device from Wolfspeed is implemented on the 30-mil RO4350B substrate to demonstrate the feasibility of the proposed out-of-band feedback stabilization technique. The PA is biased in class AB with a 100-mA quiescent current. Single-stub matching networks and 100-pF dc blocking capacitors on both the gate and drain of the transistor realize the $Z_L = 20.37 + j19.75\ \Omega$ and $Z_{\text{src}} = 49.68 + j1.25\ \Omega$ target impedances. The matching network topology is selected to ensure that no RHP poles exist within the base PA. The feedback structure $A(s)$ is implemented using a π-pad attenuator and a low-pass filter with a resonance at 511 MHz, as shown in Fig. 4. The corner frequency of the high-pass coupling networks formed by C_{IF} and L_{IF} is designed to be low (470 Hz) to ensure that the feedback network controls stability as close to dc as possible while still providing dc blocking.

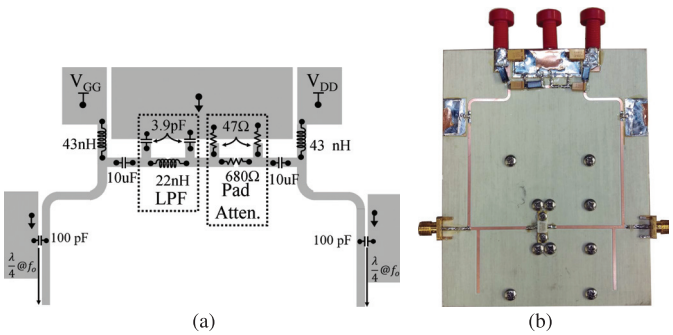

Fig. 4. Prototype amplifier as fabricated. (a) Feedback structure schematic. (b) Populated prototype amplifier board (9.14 cm × 11.43 cm).

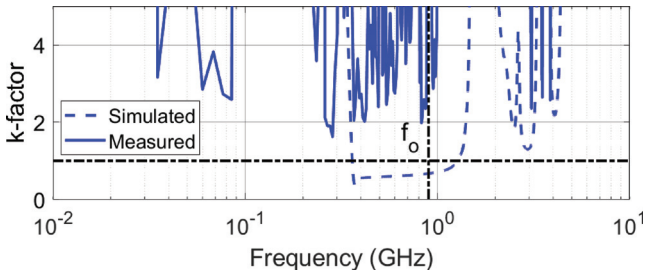

Fig. 5. Calculated k-factor of the PA with a feedback network based on S-parameter measurements and simulation.

A measured k-factor is computed from the measured S-parameters and is shown compared with simulation in Fig. 5. At high frequencies, the k-factor of the measured amplifier is consistent with simulation, but the in-band and below-band responses vary significantly. In-band, the PA has a measured k-factor greater than 1 that is most likely due to the reduced forward gain in measurement compared with simulation that can be observed in Fig. 6. At low frequencies where the feedback network operates, the measured k-factor is greater than 1, as expected. The discrepancy between measurement and simulation is due to higher measured S_{21}. The lowest k-factor occurs around 300 MHz, corresponding to the cutoff point for the stabilizing filter, and therefore the frequency at which the stabilization mechanism has the least effect on performance. Nonetheless, the measurements confirm unconditional stability produced by the feedback network.

Fig. 6 reports the gain and power added efficiency (PAE) of the stable amplifier and compares the measured results to simulation. The measured results compare favorably with the simulated results for both output power and PAE, while the measured gain is lower than simulation by 1.5 dB. When excited by a 3.84-MHz Wideband Code Division Multiple Access signal (W-CDMA) signal at 900 MHz with an average output power of 31.5 dBm, the PA remains stable with the output spectrum shown in Fig. 7.

Although direct comparison with other works is challenging due to the nature of this approach and the stability focus of this proof-of-concept work, we note that the gain reported in this letter is substantially higher than that in the state-of-the-art gallium-nitride (GaN) PAs at similar frequencies and power levels, as summarized in Table I. For example, [10] and [13] report more typical gain values for 10-W GaN PAs on the order of 15 dB at frequencies near 1 GHz. Even accounting for the device technology differences, the gain of the presented work is 6–10 dB higher than that for typical GaN PAs, while PAE is typical for the class of operation.

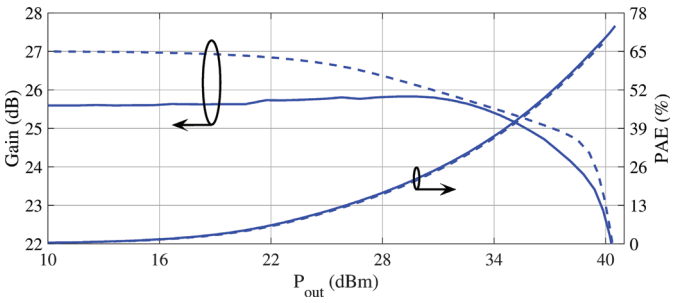

Fig. 6. Simulated and measured CW gain and PAE of the amplifier with feedback at 900 MHz with a peak envelope power at P3dB.

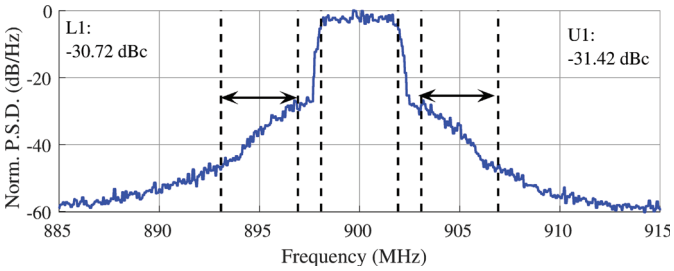

Fig. 7. Measured output W-CDMA spectrum with a peak-to-average power ratio (PAPR) of 10 dB and an average drain efficiency of 30.56%.

TABLE I
PERFORMANCE SUMMARY AND COMPARISON WITH GaN PAs IN THE LITERATURE

Ref.	Class	Freq. (MHz)	Gain (dB)	Max. Eff. (%)
[8]	E	600-1000	18-15*	PAE: 80-75*
[9]	B/J	1000-3000	13-10*	DE: 68.0-50.0*
[10]	Harm. Opt.	1250	14.5*	DE: 80*
[11]	EFJ	1200-3600	10.5-12.8	DE: 63-73
[12]	AB	700-5900	17-19*	PAE: 37-38
[13]	AB	850	14.6	PAE: 55
This work	AB	900	25.6	PAE: 73

* – read from graph

IV. CONCLUSION

This letter demonstrates a novel PA-stabilization technique that results in a high small-signal gain. Because the technique is applied as a network between the gate and drain bias lines, no lossy elements are introduced into the RF signal path. The proof-of-concept PA operates at 900 MHz with a small-signal gain of 25.6 dB, close to approximately 27-dB maximum stable power gain specified by the device manufacturer at this frequency [2], while remaining unconditionally stable over all frequencies under small-signal conditions as verified through the S-parameter measurements of the final amplifier. Large-signal measurements of the PA show typical class-AB performance, with 73% PAE at a 40-dBm continuous-wave (CW) output power.

REFERENCES

[1] I. Bahl, *Fundamentals of RF and Microwave Transistor Amplifiers*. Hoboken, NJ, USA: Wiley, 2009.

[2] *CG2H40010: 10 W, DC–6 GHz, RF Power GaN HEMT, Revision 1.1*, Cree/Wolfspeed, Durham, NC, USA, May 2018.

[3] K. W. Kobayashi, D. C. Streit, A. K. Oki, D. K. Umemoto, and T. R. Block, "A novel monolithic HEMT LNA integrating HBT-tunable active-feedback linearization by selective MBE," *IEEE Trans. Microw. Theory Techn.*, vol. 44, no. 12, pp. 2384–2391, Dec. 1996.

[4] J. Lee and J. D. Cressler, "Analysis and design of an ultra-wideband low-noise amplifier using resistive feedback in SiGe HBT technology," *IEEE Trans. Microw. Theory Techn.*, vol. 54, no. 3, pp. 1262–1268, Mar. 2006.

[5] S. Hernandez and A. Suarez, "Systematic methodology for the global stability analysis of nonlinear circuits," *IEEE Trans. Microw. Theory Techn.*, vol. 67, no. 1, pp. 3–15, Jan. 2019.

[6] J. Roberge, *Operational Amplifiers: Theory and Practice* (Massachusetts Institute of Technology Radiation Laboratory). Hoboken, NJ, USA: Wiley, 1975.

[7] J. Rollett, "Stability and power-gain invariants of linear twoports," *IRE Trans. Circuit Theory*, vol. 9, no. 1, pp. 29–32, Mar. 1962.

[8] A. A. Tanany, A. Sayed, and G. Boeck, "Broadband GaN switch mode class E power amplifier for UHF applications," in *IEEE MTT-S Int. Microw. Symp. Dig.*, Jun. 2009, pp. 761–764.

[9] T. Canning, P. J. Tasker, and S. C. Cripps, "Continuous mode power amplifier design using harmonic clipping contours: Theory and practice," *IEEE Trans. Microw. Theory Techn.*, vol. 62, no. 1, pp. 100–110, Jan. 2014.

[10] K. Rabbi *et al.*, "Highly efficient wideband harmonic-tuned power amplifier using low-pass matching network," in *Proc. 47th Eur. Microw. Conf. (EuMC)*, Oct. 2017, pp. 292–295.

[11] Z. Zhang, Z. Cheng, H. Ke, G. Liu, and S. Li, "Design of a broadband high-efficiency hybrid class-EFJ power amplifier," *IEEE Microw. Wireless Compon. Lett.*, vol. 30, no. 4, pp. 407–409, Apr. 2020.

[12] J. Lindstrand, M. Tormanen, and H. Sjoland, "A decade frequency range CMOS power amplifier for sub-6-GHz cellular terminals," *IEEE Microw. Wireless Compon. Lett.*, vol. 30, no. 1, pp. 54–57, Jan. 2020.

[13] W. Sear and T. W. Barton, "A baseband feedback approach to linearization of a UHF power amplifier," in *IEEE MTT-S Int. Microw. Symp. Dig.*, Jun. 2019, pp. 75–78.